*R*esearch in
*A*stronomy and
*A*strophysics

A model of low-frequency quasi-periodic oscillations in black hole X-ray binaries *

Zhi-Yun Wang[1,2], Chang-Yin Huang[2,3], Ding-Xiong Wang[2] and Jiu-Zhou Wang[2]

[1] School of Physics and Electronic Engineering, Hubei University of Arts and Science, Xiangyang 441053, China
[2] School of Physics, Huazhong University of Science and Technology, Wuhan 430074, China; *dxwang@mail.hust.edu.cn*
[3] School of Mathematics and Statistics, Huazhong University of Science and Technology, Wuhan 430074, China

Abstract A model of low-frequency quasi-periodic oscillations (LFQPOs) of black hole X-ray binaries (BHXBs) is proposed based on the perturbed magnetohydrodynamic equations of an accretion disk. It turns out that the LFQPO frequencies of some BHXBs can be fitted by the frequencies of the toroidal Alfvén wave oscillation corresponding to the maximal radiation flux. In addition, the positive correlation of the LFQPO frequencies with the radiation flux from an accretion disk is well interpreted.

Key words: accretion, accretion disks — black hole physics — magnetic fields — stars: individual (XTE J1550–564, GRO J1655–40)

1 INTRODUCTION

It is well known that quasi-periodic oscillations (QPOs) have been widely observed in some X-ray binaries, whose compact object is either a neutron star or a black-hole, and QPOs play an essential role as a potentially important tool for studying the strong gravitational field and understanding the physical processes of X-ray states (Done et al. 2007). Among ∼20 black hole X-ray binaries (BHXBs), the low-frequency QPOs (LFQPOs) with frequency ranging from a few mHz to 30 Hz have been detected on one or more occasions for 14 systems in the hard state and in the steep power-law (SPL) state (McClintock & Remillard 2006). Almost all the LFQPOs have some common properties, with features usually remaining relatively stable for days or weeks.

A number of theoretical models have been proposed to explain the physical mechanisms of LFQPOs. Tagger & Pellat (1999) suggested that LFQPOs observed in low-mass BHXBs can be interpreted by accretion-ejection instability. Titarchuk & Osherovich (2000) considered that the LFQPOs are caused by the global disk oscillation in the direction normal to the disk, and these oscillations arise from the gravitational interaction between the central compact object and the disk. O'Neill et al. (2011) proposed that LFQPOs are related to the quasi-periodic behavior in global magnetohydrodynamic (MHD) dynamos. Cabanac et al. (2010) presented an oscillating corona due to a magneto-acoustic wave propagating in the corona and producing multiple QPOs. Kato (2008)

proposed that the one-armed c-mode low frequency oscillations of the disk are one of the possible candidates of LFQPOs based on a resonantly-excited disk-oscillation model. In addition, the relativistic precession model was first presented by Stella & Vietri (1998), who suggested that LFQPOs are the result of some modulation of Lense-Thirring precession. Later, Schnittman et al. (2006) and Ingram et al. (2009); Ingram & Done (2012) developed this model, and successfully explained the variability properties of BHXBs. However, there has been no consensus on the physical nature of LFQPOs.

On the other hand, it has been found that LFQPO frequencies exhibit a strong positive correlation with disk flux from observations. For example, LFQPO frequencies of XTE J1550–564 (33 observations during 1998.9–1999.4), GRO J1655–40 (38 observations during 2005.2.17–2005.3.6) and H1743–322 (20 observations during 2003.3.28–2003.5.22) display a roughly linear relation with disk flux, when they are in the hard and intermediate states with frequencies in the range 1–7 Hz, 0.01–2.5 Hz and 2–5 Hz, respectively (Remillard & McClintock 2006; McClintock et al. 2009; Sobczak et al. 2000; Shaposhnikov et al. 2007). Similar quasi-linear relations of LFQPO frequencies with disk flux have been found for GRS 1915+105 (32 observations during 1996.10.29–1998.10.7) in the range 1–15 Hz (Markwardt et al. 1999; Sobczak et al. 2000; Muno et al. 2001) and for XTE J1748–288 (92 observations during 1998.7.13–1998.9.26) in the range 20–30 Hz (Revnivtsev et al. 2000). From the duration of the above outbursts, we can find that this positive correlation between the LFQPO frequencies and disk flux has long timescales. It is noted that the QPO observed in XTE J1550–564 during its 1998 outburst shows a correlation between absolute rms amplitude and mean source flux over timescales shorter than ~ 3 ks (Heil et al. 2011), so this relation also holds on short timescales. However, the origin of the correlation between LFQPO frequency and disk flux of BHXBs remains elusive.

If the magnetic field is taken into account in the accretion disk, a torsional Alfvén wave can be generated by the rotational drag of space (Koide et al. 2002). We consider a toroidal magnetic field existing in a rotational accretion disk, in which an Alfvén wave oscillation propagates along toroidal magnetic field lines due to the perturbation of radial velocity of the accreting matter. Thus the Alfvén wave oscillation will influence the transformation of angular momentum and the radiation flux from the inner disk. Although some researchers suggested that the QPOs of low mass BHXBs arise from Alfvén waves (Zhang 2004; Shi & Li 2010; Shi 2011), the association of Alfvén wave oscillation with LFQPOs has not been discussed.

In this paper, we adopt a binary system consisting of a Kerr black hole surrounded by a weakly magnetized relativistic thin disk to derive the Alfvén wave frequency based on the perturbed MHD equations, and the LFQPO frequency is fitted by the frequency of the Alfvén wave propagating in a specific circular orbit of the accretion disk, which corresponds to the maximum radiation flux. In addition, we propose a thin disk model with some corona floating above the disk to well interpret the positive correlation of the LFQPO frequencies with disk flux.

This paper is organized as follows. In Section 2, we present a description of our model, and derive the formula for Alfvén wave frequency and radiation flux. In Section 3, we fit the LFQPO frequencies of several BHXBs, and fit the positive correlation of LFQPO frequency with the disk flux for two BHXBs, XTE J1550–564 and GRO 1655–40. Finally, in Section 4, we discuss the results obtained in our model.

2 MODEL DESCRIPTION

2.1 Alfvén Wave Oscillations in an Accretion Disk

We consider a geometrically thin, optically thick, non-self-gravitating perfect fluid disk, which is magnetized and isothermal, and rotating around a BH. It is assumed that the magnetic pressure is much less than the total pressure ($p_{\mathrm{mag}} \ll p$), which is a good approximation to a thin Keplerian disk

(Li 2002). The disk dynamics are governed by the ideal MHD equations given as follows.

$$\frac{\partial \rho}{\partial t} + \nabla \cdot (\rho \boldsymbol{v}) = 0 \,, \tag{1}$$

$$\frac{\partial \boldsymbol{v}}{\partial t} + \boldsymbol{v} \cdot \nabla \boldsymbol{v} + \frac{1}{\rho} \nabla p + \nabla \Phi + \frac{1}{4\pi\rho} \boldsymbol{B} \times (\nabla \times \boldsymbol{B}) = 0 \,. \tag{2}$$

The magnetic field $\boldsymbol{B}$ satisfies the induction equation in the MHD approximation, and it reads

$$\frac{\partial \boldsymbol{B}}{\partial t} - \nabla \times (\boldsymbol{v} \times \boldsymbol{B}) = 0 \,, \tag{3}$$

and

$$\nabla \cdot \boldsymbol{B} = 0 \,. \tag{4}$$

The quantities ρ, $\boldsymbol{v}$ and p in Equations (1) and (2) denote mass density, velocity and pressure of plasma, respectively. The Pseudo-Kerr potential (Mukhopadhyay 2002) Φ is adopted to simulate the effects of general relativity, and it reads

$$\nabla \Phi = -\frac{c^4 (r^2 - 2a_* \sqrt{r} + a_*^2)^2}{GMr^3 [\sqrt{r}(r-2) + a_*]^2} \,, \tag{5}$$

where r is the distance between the plasma to the center of the BH ($r = R/R_{\rm g}$), and $R_{\rm g} \equiv GM/c^2$ is the gravitational radius. The quantities M, G and c denote respectively the BH mass, gravitational constant and speed of light, and J and $a_* = J/(GM/c^2)$ represent the BH angular momentum and the dimensionless spin, respectively.

The Keplerian angular velocity in the frame of a Pseudo-Kerr potential is derived by Shafee et al. (2008) as follows,

$$\Omega_k = \frac{c^3 (r^2 - 2a_* \sqrt{r} + a_*^2)}{GMr^2 [\sqrt{r}(r-2) + a_*]} \,. \tag{6}$$

The perturbed physical quantities in MHD equations can be written as

$$p = p_0 + p' \,, \qquad \rho = \rho_0 + \rho' \,, \qquad \boldsymbol{v} = \boldsymbol{v}_0 + \boldsymbol{v}' \,, \qquad \boldsymbol{B} = \boldsymbol{B}_0 + \boldsymbol{B}' \,, \tag{7}$$

where the subscript '0' and superscript '′' denote the equilibrium and perturbation values, respectively. Assuming that all the perturbations are small enough, i.e. $\rho_0 \gg \rho'$, $p_0 \gg p'$, $v_0 \gg v'$, $B_0 \gg B'$, we can neglect their products in second and higher orders. Substituting Equations (4) and (7) into Equations (1)–(3), we have the linearized MHD perturbation equations as follows,

$$\frac{\partial \rho'}{\partial t} + \rho_0 (\nabla \boldsymbol{v}') + (\nabla \rho') \cdot \boldsymbol{v}_0 = 0 \,, \tag{8}$$

$$\frac{\partial \boldsymbol{v}'}{\partial t} + \boldsymbol{v_0} \cdot (\nabla \boldsymbol{v}') + \frac{c_s^2}{\rho_0} \nabla \rho' + \frac{\boldsymbol{B_0}}{4\pi\rho_0} \times (\nabla \times \boldsymbol{B}') = 0 \,, \tag{9}$$

$$\frac{\partial \boldsymbol{B}'}{\partial t} - \nabla \times (\boldsymbol{v}' \times \boldsymbol{B_0}) = 0 \,. \tag{10}$$

From the vertical equilibrium assumption of the accretion disk, the half-height (H) of the disk can be written as (Mukhopadhyay 2003),

$$H = c_{\rm s}/\Omega_k \,, \tag{11}$$

where $c_{\rm s} = \sqrt{p/\rho}$ is the sound speed.

Incorporating Equations (8)–(10), we have the equation for the velocity perturbation as follows,

$$\frac{\partial^2 \boldsymbol{v}'}{\partial t^2} + \boldsymbol{v_0} \cdot \nabla\left(\frac{\partial \boldsymbol{v}'}{\partial t}\right) + c_{\mathrm{s}}^2 \nabla(\nabla \cdot \boldsymbol{v}') + \boldsymbol{v}_{\mathrm{A}} \cdot \nabla \times [\nabla \times (\boldsymbol{v}' \times \boldsymbol{v}_{\mathrm{A}})] = 0\,, \tag{12}$$

where $\boldsymbol{v}_{\mathrm{A}} = \frac{\boldsymbol{B_0}}{\sqrt{4\pi\rho_0}}$ is Alfvén velocity, being defined as

$$\boldsymbol{v}_{\mathrm{A}} = \frac{|\boldsymbol{B_0}|}{\sqrt{4\pi\rho_0}} = \sqrt{\beta}c_{\mathrm{s}} = \sqrt{\beta}H\Omega_k\,, \tag{13}$$

where $\beta = p_{\mathrm{mag}}/p$ is defined as the ratio of magnetic pressure to total pressure.

In order to fit LFQPO frequencies by invoking Alfvén wave propagating in an accretion disk, we express the perturbed velocity as follows,

$$\boldsymbol{v}' = \boldsymbol{v}'\mathrm{e}^{i(\boldsymbol{k}\cdot\boldsymbol{\xi}-\omega t)}\,, \tag{14}$$

where ω, $\boldsymbol{\xi}$ and $\boldsymbol{k}$ are the perturbation frequency, the displacement vector and the wavenumber vector, respectively. In cylindrical coordinates the wavenumber vector is $\boldsymbol{k} = k_r\hat{\boldsymbol{r}} + k_\varphi\hat{\boldsymbol{\varphi}} + k_z\hat{\boldsymbol{z}}$, where k_r, k_φ, k_z represent the radial, azimuthal and vertical components, respectively. Substituting Equation (14) into Equation (12), we have

$$-\omega^2 \boldsymbol{v}' - \omega k\boldsymbol{v_0}\cdot\boldsymbol{v}' + (c_{\mathrm{s}}^2 + v_{\mathrm{A}}^2)(\boldsymbol{k}\cdot\boldsymbol{v}')\boldsymbol{k} + (\boldsymbol{v}_{\mathrm{A}}\cdot\boldsymbol{k})\cdot[(\boldsymbol{v_A}\cdot\boldsymbol{k})\boldsymbol{v}' - (\boldsymbol{v}_{\mathrm{A}}\cdot\boldsymbol{v}')\boldsymbol{k} - (\boldsymbol{k}\cdot\boldsymbol{v}')\boldsymbol{v}_{\mathrm{A}}] = 0\,. \tag{15}$$

Considering that the Alfvén wave is a transverse wave, being transported along the magnetic field line, we have $\boldsymbol{k}\|\boldsymbol{B_0}\|\boldsymbol{v_0} \perp \boldsymbol{v}'$, and Equation (14) is simplified as

$$k^2 v_{\mathrm{A}}^2 - \omega^2 = 0\,, \tag{16}$$

where the symbols $\|$ and $\perp$ denote parallel and perpendicular directions, respectively. Thus the angular velocity of the perturbation is related to the Alfvén velocity v_{A} as follows,

$$\omega = kv_{\mathrm{A}} = k\sqrt{\beta}c_{\mathrm{s}}\,. \tag{17}$$

For a thin magnetized accretion disk, Armitage & Natarajan (1999) presented that the dominant field component is toroidal with saturation occurring when $p_{\mathrm{mag}}\ll p$. So we assume that the unperturbed flow is axisymmetric, and only the toroidal magnetic field exists in the equilibrium state in the accretion disk, i.e. $\boldsymbol{B_0} = B_\varphi\hat{\varphi}$. Thus a small perturbation of radial velocity of fluid due to accretion of the black hole gives rise to the oscillation of the magnetic field B_φ, and results in the Alfvén wave oscillation propagating in the toroidal direction in the disk. For the characteristic wavelength $\lambda \sim R$, the toroidal wave number $k_\varphi \sim 2\pi/R$ (Shi & Li 2010), and the angular velocity of the perturbation can be written as

$$\omega = k_\varphi\sqrt{\beta}c_{\mathrm{s}} = 2\pi\frac{H}{R}\sqrt{\beta}\Omega_k\,. \tag{18}$$

Inspecting Equation (18) we find that ω is much less than the Keplerian angular velocity Ω_k in the thin disk due to the disk scale height H being much less than disk radius R, and this perturbation frequency provides a possibility for fitting LFQPO frequencies of BHXBs.

2.2 Relation between LFQPO Frequency and Perturbation Frequency

First of all, we intend to clarify the relation between LFQPO frequency and the perturbation frequency. The disk angular velocity can be regarded as the Keplerian angular velocity, i.e. $\Omega = \Omega_k$, provided that the radial magnetic force can be neglected. This result can occur only if the toroidal magnetic field exists without a vertical electric current in the thin disk.

The rate of energy generation per unit area of one side of the disk is given by (Shakura & Sunyaev 1973; Novikov & Thorne 1973; Gierliński et al. 1999; Shafee et al. 2008),

$$Q(R) = -RH\alpha p\frac{d\Omega_R}{dR} = -\frac{\dot{M}(R^2\Omega_R - R_{\mathrm{ms}}^2\Omega_{\mathrm{ms}})}{4\pi R} \cdot \frac{d\Omega_R}{dR}, \tag{19}$$

where $\dot{M}$ and α are respectively the mass accretion rate and viscosity parameter; Ω_R and Ω_{ms} denote respectively the angular velocity at R and the inner edge of the disk. The radius R_{ms} of the innermost stable circular orbit (ISCO) of the accretion disk varies with a_* in the Pseudo-Kerr potential, and Mukhopadhyay (2002) showed that r_{ms} ($r_{\mathrm{ms}} = R_{\mathrm{ms}}/R_{\mathrm{g}}$) satisfies the following equation

$$-3a_*^4 + 14a_*^3\sqrt{r_{\mathrm{ms}}} + (r_{\mathrm{ms}} - 6)r_{\mathrm{ms}}^3 + 6a_*r_{\mathrm{ms}}^{3/2}(r_{\mathrm{ms}} + 2) - 2a_*^2 r_{\mathrm{ms}}(r_{\mathrm{ms}} + 11) = 0. \tag{20}$$

It is easy to find that the ISCO moves toward the BH with increasing a_* as shown in Figure 1. Thus the local radiation flux $F(r)$ can be written as

$$F(r) = \frac{\dot{M}c^6}{8\pi G^2 M^2 r^4}g(r, r_{\mathrm{ms}}, a_*), \tag{21}$$

where we have $r = R/R_{\mathrm{g}}$, and

$$\begin{aligned}
g(r, r_{\mathrm{ms}}, a_*) = & (2r^2\sqrt{r_{\mathrm{ms}}} - r^2\sqrt{r_{\mathrm{ms}}^3} - r^2 a_* + 2a_*\sqrt{rr_{\mathrm{ms}}^3} - a_*^2\sqrt{r_{\mathrm{ms}}^3} + r_{\mathrm{ms}}^2\sqrt{r^3} - 2r_{\mathrm{ms}}^2\sqrt{r} \\
& + r_{\mathrm{ms}}^2 a_* - 2a_*\sqrt{r^3 r_{\mathrm{ms}}} + a_*^2\sqrt{r^3})(12\sqrt{r^5}a_* - 3r^4 + 16a_*^2 r - 16a_*\sqrt{r^3} - 7r^2 a_*^2 \\
& + 2r^3 - 4a_*^3\sqrt{r})/[\sqrt{r}(\sqrt{r^3} - 2\sqrt{r} + a_*)^3(\sqrt{r_{\mathrm{ms}}^3} - 2\sqrt{r_{\mathrm{ms}}} + a_*)]. \tag{22}
\end{aligned}$$

By using Equations (20) and (21), we plot the curves of local flux $F(r)$ versus r as shown in Figure 1, and we find that the radiation flux is dominantly produced in the inner disk; it varies non-monotonically with r, attaining its peak value at r_d close to the ISCO. In addition, as shown in Figure 1, we find that the peak value of $F(r)$ is greater, and the location of r_d is closer to the ISCO for a greater BH spin.

Inspecting Equations (18)–(21), we can find that the radiation flux is directly caused by the angular momentum transport. For a magnetized thin accretion disk, numerical simulations have shown that the angular momentum transport is dominated by Maxwell stresses (Hawley et al. 1995; Brandenburg et al. 1995; Stone et al. 1996), and the magnetic contribution to the viscosity parameter α exceeds fluid stresses by an order of magnitude, so that $\alpha \simeq \alpha_{\mathrm{magnetic}}$ (Armitage & Natarajan 1999). So in low mass X-ray binaries the high energy X-ray radiation is generated mainly from the interaction of the plasma with the magnetic field, and the change of the magnetic field could modulate the X-ray flux (Shi 2011). Thereby the oscillations of the toroidal Alfvén wave may lead to the QPOs. Since the strongest influence of the perturbation on luminosity corresponds to the maximum radiation flux $F_{\mathrm{max}}(r = r_d)$, the perturbation frequency at r_d can be regarded as the LFQPO frequency.
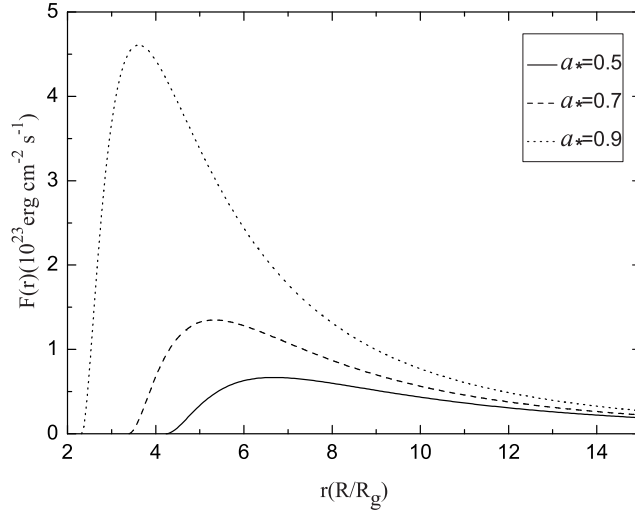
Fig. 1 Curves of local radiation flux $F(r)$ versus r with the given values of a_* ($M = 10M_\odot$ and $\dot{M} = 0.1\dot{M}_{\mathrm{Edd}}$, where $\dot{M}_{\mathrm{Edd}}$ is the Eddington accretion rate).

3 FITTING LFQPOS OF BHXBS

In this section we intend to fit the LFQPOs of several BHXBs based on the above relation between LFQPO frequency and the perturbation frequency. In addition, the positive correlation between LFQPO frequency and disk flux can be well interpreted based on our model.

We consider a geometrically thin, optically thick accretion disk with a corona floating above given by Gierliński et al. (1999). In the inner region of weak magnetic fields, the gas pressure and magnetic pressure can be neglected, and the total pressure is

$$p \simeq p_{\mathrm{rad}} = \frac{4\sigma}{3c}T_{\mathrm{c}}\,, \tag{23}$$

where σ is the Stefan-Boltzmann constant, and the quantity T_{c} is the temperature of the central disk, which is determined by the equilibrium between the radiation cooling in the vertical direction and the energy generated by the viscous dissipation. We assume that a fraction q of the total energy generated by the viscous process is emitted from the disk, and the remainder is dissipated in the corona. This energy equation is written as (Frank et al. 2002; Gierliński et al. 1999)

$$\frac{4\sigma}{3\tau}T_{\mathrm{c}}^4 = qF(r)\,. \tag{24}$$

The parameter τ in Equation (24) is the opacity for electron scattering, and it reads

$$\tau \cong \rho H \sigma_{\mathrm{T}}/m_{\mathrm{p}}\,, \tag{25}$$

where σ_{T} and m_{p} denote the Thomson cross-section and proton mass, respectively. Incorporating Equation (11) with Equations (23)–(25), we obtain

$$H = \frac{q\sigma_{\mathrm{T}}}{m_{\mathrm{p}}c(\Omega_k)^2}F(r)\,. \tag{26}$$

The Eddington accretion rate $\dot{M}_{\mathrm{Edd}}$ can be written as

$$\dot{M}_{\mathrm{Edd}} = 2\pi R_{\mathrm{ms}}m_{\mathrm{p}}c/\eta\sigma_{\mathrm{T}}\,, \tag{27}$$

Table 1 Fitting LFQPO Frequencies of X-ray BHBs

Source	ν_{QPO}^a	m_{BH}^b	a_*^b	$\beta = p_{\mathrm{mag}}/p$	$\dot{m}$
GRO J1665−40	0.1−28	6.2	0.7		0.00086−0.24
XTE J1550−564	0.1−10	9.1	0.34	0.01	0.0023−0.23
GRS 1915+105	0.001−10	15.0	0.975		0.00007−0.07
4U 1543−47	7	9.4	0.8		0.073

Notes: [a]Remillard & McClintock (2006); [b]Narayan & McClintock (2012).

where η is the accretion efficiency, whose value is 0.1 for a black hole. Substituting Equations (6), (21) and (27) into Equation (26), we have

$$H = 3.7 \times 10^5 m_{\mathrm{BH}} \dot{m} q \frac{r_{\mathrm{ms}}(\sqrt{r^3} - 2\sqrt{r} + a_*)^2}{(2a_*\sqrt{r} - r^2 - a_*^2)^2} g(r, r_{\mathrm{ms}}, a_*), \qquad (28)$$

where we define $m_{\mathrm{BH}} \equiv M/M_\odot$ and $\dot{m} \equiv \dot{M}/\dot{M}_{\mathrm{Edd}}$.

Combining Equations (6), (18) and (28), we have the perturbation frequency as a function of disk radius r, and we derive the expression for LFQPO frequency by setting $r = r_d$ as follows,

$$\nu_{\mathrm{QPO}} = \frac{\omega}{2\pi} = 5.1 \times 10^5 \frac{\sqrt{\beta}\dot{m}q}{m_{\mathrm{BH}}} \frac{r_{\mathrm{ms}}(\sqrt{r_d^3} - 2\sqrt{r_d} + a_*)}{r_d^3(2a_*\sqrt{r_d} - r_d^2 - a_*^2)} g(r_d, r_{\mathrm{ms}}, a_*). \qquad (29)$$

From Equation (29) we find that the LFQPO frequency is proportional to the accretion rate $\dot{m}$, but it is inversely proportional to the BH mass m_{BH}. Based on the above results we can fit some LFQPO frequencies of several BHXBs with the given BH mass by adjusting the mass accretion rate and the intensity of the magnetic field β, and the main results are summarized as follows.

First, the theoretical values of the LFQPO frequencies are in accordance with the observed ones with appropriate values of $\dot{m}$ and β. We assume that the dissipation in the corona can be neglected ($q = 1$), and $\beta = p_{\mathrm{mag}}/p = 0.01$; the fitting results are listed in Table 1.

Second, the observed strong positive correlation between the LFQPO frequencies and the disk flux can be interpreted very well based on our model. We assume that the disk locally emits a blackbody spectrum, of which a fraction $1 - p_{\mathrm{sc}}$ is scattered in the corona, and the disk luminosity is (Gierliński et al. 1999)

$$L_s = p_{\mathrm{sc}} q \eta \dot{M} c^2 = \frac{2\pi D^2 F_s}{\cos i}, \qquad (30)$$

where i and D are the inclination of the disk and the source distance to the observer, respectively. The quantity $(1 - p_{\mathrm{sc}})$ is the fraction of the disk emission which is not scattered by the corona, and F_s is the observed disk flux. Combining Equations (29) and (30), we obtain the relation between the LFQPO frequency and the observed disk flux F_s as follows.

$$\nu_{\mathrm{QPO}} = 2.5 \times 10^{-33} \frac{\sqrt{\beta}F_s D^2}{m_{\mathrm{BH}}^2 p_{\mathrm{sc}} \cos i} \frac{r_{\mathrm{ms}}(\sqrt{r_d^3} - 2\sqrt{r_d} + a_*)}{r_d^3(2a_*\sqrt{r_d} - r_d^2 - a_*^2)} g(r_d, r_{\mathrm{ms}}, a_*). \qquad (31)$$

From Equation (31) we find that the LFQPO frequency has a positive correlation with the observed disk flux. For XTE J1550–564 (outburst in 1998) and GRO J1655–40 (outburst in early 2005), the values of p_{sc} are about 15% (Sobczak et al. 2000) and 10% (Shaposhnikov et al. 2007), respectively, and they stay constant in the hard states. Therefore their disk fluxes have a linear relation with LFQPO frequencies.

For a given source, the values of r_{ms} and r_d can be obtained by resolving Equations (20) and (21), and the values of the parameters (such as $m_{\mathrm{BH}}, a_*, D, i$, and p_{sc}) are available in the literatures. Substituting all the parameters into the Equation (31), we can derive the LFQPO frequency
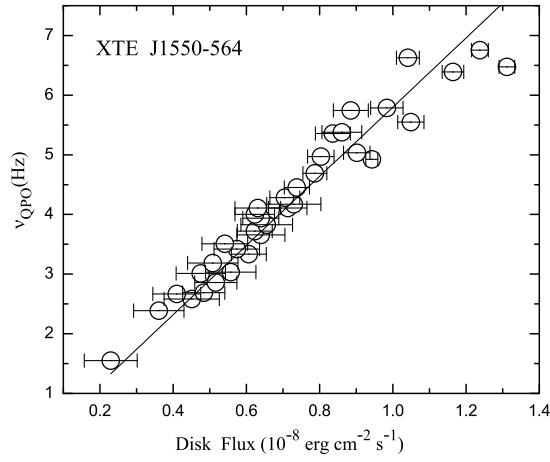
Fig. 2 Fitting the relation between the disk flux and LFQPO frequency for XTE J1550–564. The observed data are taken from fig. 2 of Sobczak et al. (2000), and the flux errors are corrected based on McClintock et al. (2009).

Table 2 Fitting Parameters for LFQPO Frequencies of XTE J1550–564 and GRO J1655–40

Source	Input				Output			Fitting parameter	χ^2 (dof)
	m_{BH}	a_*	D (kpc)	i	p_{sc}	r_{ms}	r_d	$\beta = p_{\mathrm{mag}}/p$	
XTE J1550−564	9.1	0.34	4.38	75°	0.15	4.83	7.64	0.0105 ± 0.0003	44.9(32)
GRO J1665−40	6.3	0.7	3.2	70°	0.1	3.39	5.33	0.0159 ± 0.0005	61.2(37)

Notes: The values of input parameters (m_{BH}, a_*, D, i) are adopted from Narayan & McClintock (2012). The quantities of r_{ms} and r_d are computed by using Equations (20) and (21).

corresponding to disk flux F_s and the magnetic field parameter β as follows,

$$\nu_{\mathrm{QPO}} = f(\beta)F_s \,, \tag{32}$$

where $f(\beta)$ is a function of β. The measured values of LFQPO frequency and disk flux are ν_i and F_i ($i = 1, 2, \cdots, N$, the number of the observed data), of which the errors are $\epsilon_{\nu i}$ and $\epsilon_{F i}$, respectively. We adopt the Nukers' estimate (Tremaine et al. 2002) based on minimizing

$$\chi^2 \equiv \sum_{i=1}^{N} \frac{(\nu_i - f(\beta)F_i)^2}{\epsilon_{\nu i}^2 + f^2(\beta)\epsilon_{F i}^2} \,. \tag{33}$$

Using the Nukers' estimate, we can derive the values of the best fitting parameter β for XTE J1550–564 and GRO J1655–40, which are presented in Table 2. The values of reduced χ^2 per degree of freedom are less than 2 for both sources, indicating that the LFQPO frequency has an approximately linear relation with disk flux as shown in Figures 2 and 3 for XTE J1550–564 and GRO J1655–40, respectively.

4 DISCUSSION

In this paper, we propose that the LFQPOs in BHXBs can be interpreted by invoking the toroidal Alfvén wave oscillations located at the disk radius with maximal radiation flux. It turns out that the LFQPO frequencies of several BHXBs can be well fitted based on our model. In addition, the
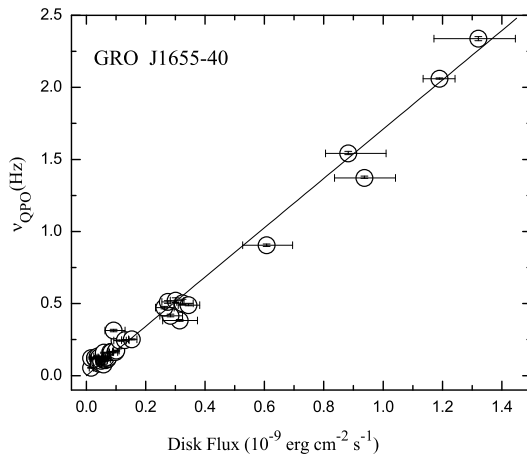
Fig. 3 Fitting the relation between the disk flux and LFQPO frequency for GRO J1655–40 ($m_{BH} = 6.2$, $\beta = 0.6$, $D = 3.2$ kpc, $i = 70°$). The observed data are taken from fig. 15 of Shaposhnikov et al. (2007).

positive correlation between the LFQPO frequencies and the disk flux of XTE J1550–564 and GRO J1655–40 is also well fitted. According to the argument given in Sections 2 and 3, we find that the positive correlation between LFQPO frequency and the disk flux can be understood, because both the perturbation frequency of the toroidal Alfvén wave and LFQPO frequency increase with an increasing accretion rate. It is noted that this correlation only holds in hard states, when the disk fraction stays constant. Thus our model provides an explanation for the fact that LFQPOs are primarily observed in the power law part of spectra from BHXBs (Życki & Sobolewska 2005).

We adopt a thin disk with a corona floating above, which is different from the model of a corona's interior to a truncated disk as given by Done et al. (2007). The truncated disk is not compatible with our model because it is difficult to determine the location of maximal radiation flux. If an Alfvén wave from a truncated disk is used to interpret QPOs, a certain appropriate location for the Alfvén wave propagation must be found, e.g. Shi (2011) used Alfvén wave oscillation at the transition radius to explain HFQPOs of low mass X-ray binaries.

Although LFQPOs are interpreted successfully by invoking perturbed Alfvén wave oscillation, it seems difficult to explain high frequency QPOs (HFQPOs) of BHXBs. This could imply that the physical origins of LFQPOs and HFQPOs are different. HFQPOs in BHXBs have been successfully explained by the magnetic hot spots model (Wang et al. 2003, 2005) and resonance mode (Abramowicz & Kluźniak 2001; Huang et al. 2010); the HFQPO frequencies are sensitive to BH mass and spin, but they seem to not be directly related to the accretion rate or disk flux. It is noted that HFQPOs may be triggered by the instability of accretion disk oscillation (Tagger & Varnière 2006; Caunt & Tagger 2001). We also notice that the instability occurs in the toroidal Alfvén wave oscillation, and the oscillation frequency is comparable to the HFQPO frequency, provided that the accretion rate and the magnetic field are great enough. This result motivates us to explore the relation between HFQPOs and the instability of Alfvén wave oscillation in our future work.

References

Abramowicz, M. A., & Kluźniak, W. 2001, A&A, 374, L19

Armitage, P. J., & Natarajan, P. 1999, ApJ, 523, L7

Brandenburg, A., Nordlund, A., Stein, R. F., & Torkelsson, U. 1995, ApJ, 446, 741

Cabanac, C., Henri, G., Petrucci, P.-O., et al. 2010, MNRAS, 404, 738

Caunt, S. E., & Tagger, M. 2001, A&A, 367, 1095

Done, C., Gierliński, M., & Kubota, A. 2007, A&A Rev., 15, 1

Frank, J., King, A., & Raine, D. J. 2002, Accretion Power in Astrophysics: Third Edition (Cambridge, UK: Cambridge Univ. Press)

Gierliński, M., Zdziarski, A. A., Poutanen, J., et al. 1999, MNRAS, 309, 496

Hawley, J. F., Gammie, C. F., & Balbus, S. A. 1995, ApJ, 440, 742

Heil, L. M., Vaughan, S., & Uttley, P. 2011, MNRAS, 411, L66

Huang, C.-Y., Gan, Z.-M., Wang, J.-Z., & Wang, D.-X. 2010, MNRAS, 403, 1978

Ingram, A., & Done, C. 2012, MNRAS, 419, 2369

Ingram, A., Done, C., & Fragile, P. C. 2009, MNRAS, 397, L101

Kato, S. 2008, PASJ, 60, 889

Koide, S., Shibata, K., Kudoh, T., & Meier, D. L. 2002, Science, 295, 1688

Li, L.-X. 2002, ApJ, 567, 463

Markwardt, C. B., Swank, J. H., & Taam, R. E. 1999, ApJ, 513, L37

McClintock, J. E., & Remillard, R. A. 2006, Black hole binaries, eds. W. H. G. Lewin, & M. van der Klis, 157

McClintock, J. E., Remillard, R. A., Rupen, M. P., et al. 2009, ApJ, 698, 1398

Mukhopadhyay, B. 2002, ApJ, 581, 427

Mukhopadhyay, B. 2003, ApJ, 586, 1268

Muno, M. P., Remillard, R. A., Morgan, E. H., et al. 2001, ApJ, 556, 515

Narayan, R., & McClintock, J. E. 2012, MNRAS, 419, L69

Novikov, I. D., & Thorne, K. S. 1973, in Black Holes (Les Astres Occlus), eds. C. Dewitt, & B. S. Dewitt, 343

O'Neill, S. M., Reynolds, C. S., Miller, M. C., & Sorathia, K. A. 2011, ApJ, 736, 107

Remillard, R. A., & McClintock, J. E. 2006, ARA&A, 44, 49

Revnivtsev, M. G., Trudolyubov, S. P., & Borozdin, K. N. 2000, MNRAS, 312, 151

Schnittman, J. D., Homan, J., & Miller, J. M. 2006, ApJ, 642, 420

Shafee, R., Narayan, R., & McClintock, J. E. 2008, ApJ, 676, 549

Shakura, N. I., & Sunyaev, R. A. 1973, A&A, 24, 337

Shaposhnikov, N., Swank, J., Shrader, C. R., et al. 2007, ApJ, 655, 434

Shi, C.-S. 2011, RAA (Research in Astronomy and Astrophysics), 11, 1327

Shi, C.-S., & Li, X.-D. 2010, ApJ, 714, 1227

Sobczak, G. J., McClintock, J. E., Remillard, R. A., et al. 2000, ApJ, 531, 537

Stella, L., & Vietri, M. 1998, ApJ, 492, L59

Stone, J. M., Hawley, J. F., Gammie, C. F., & Balbus, S. A. 1996, ApJ, 463, 656

Tagger, M., & Pellat, R. 1999, A&A, 349, 1003

Tagger, M., & Varnière, P. 2006, ApJ, 652, 1457

Titarchuk, L., & Osherovich, V. 2000, ApJ, 542, L111

Tremaine, S., Gebhardt, K., Bender, R., et al. 2002, ApJ, 574, 740

Wang, D.-X., Ma, R.-Y., Lei, W.-H., & Yao, G.-Z. 2003, ApJ, 595, 109

Wang, D.-X., Ye, Y.-C., Yao, G.-Z., & Ma, R.-Y. 2005, MNRAS, 359, 36

Zhang, C. 2004, A&A, 423, 401

Życki, P. T., & Sobolewska, M. A. 2005, MNRAS, 364, 891